附件一

行政院國家科學委員會補助專題研究計畫 ■ 成 果 報 告 □期中進度報告

拍翼式微型自主飛行系統-子計畫二 ：

拍翼型飛行器之自主飛行動力學及姿態控制探討

計畫類別：□ 個別型計畫　　■ 整合型計畫
計畫編號：NSC 96-2221-E-032-015-
執行期間： 2007 年 8 月 1 日至 2008 年 7 月 31 日

計畫主持人：蕭富元 博士
共同主持人：
計畫參與人員： 陳正霖、楊澤明

成果報告類型(依經費核定清單規定繳交)：■精簡報告　□完整報告

本成果報告包括以下應繳交之附件：
□赴國外出差或研習心得報告一份
□赴大陸地區出差或研習心得報告一份
■出席國際學術會議心得報告及發表之論文各一份
□國際合作研究計畫國外研究報告書一份

處理方式：除產學合作研究計畫、提升產業技術及人才培育研究計畫、列管計畫及下列情形者外，得立即公開查詢
□涉及專利或其他智慧財產權，□一年□二年後可公開查詢

執行單位：淡江大學航空太空工程學系

中 華 民 國 九十七 年 十 月 十五 日

Dynamics of Flapping Micro-Aerial Vehicles

T.M. Yang*and F.Y. Hsiao†

Abstract

The dynamics of flapping wing micro aerial vehicles (MAVs) is studied in this paper. The MEMS Laboratory in Tamkang University has been developing flapping wing MAVs for several years. Based on the developed flapping wing MAV we study its dynamics and compare our results with flight test data. Although several papers have discussed similar topics previously, using our flight test data we demonstrate the validity of some assumptions and our derivations. We also propose a claim that links the time-average aerodynamical forces to the wind tunnel test database, so that a flapping MAV can be analyzed in the same methodology as what we have done to a fixed-wing aircraft. Flight test data and numerical simulations are also provided to demonstrate the validity of our results.

1 Introduction

Flight in flapping is a very efficient way to transport a unit of mass over a unit of distance, even thouth it requires extremely high power output[5]. For this reason, it is an interesting field and a new generation technology for the flight configuration. There are two kinds of flight configuration that is investigated in the literatures on natural flapping flight: Bird-like flight and Insect-like flight. The focus of this paper is on bird-like flight. The bird-like aerial robot we are investigating is developed by the TKU MEMS LAB in the recent years.

The aerodynamics performance in flapping animals consists of delayed stall, rotational circulation and wake capture [10]. These phenomenon and their functions can be explained by experiments and theories. However, complete and exact analysis of the flapping flight is not available because of the aerodynamic and mechanical complexity. As a result, In Ref. [4] Kim developed a smart flapping wing with a macro-fiber compositers (MFC) actuator to mimic the flying mechanism to measure the aerodynamic forces of flapping devices in wind tunnel test. Furthermore, In Ref. [7] Rakotomamonjy investigates the optimization of the flapping kinematics of the wing. In the full dynamic model of flapping MAV, Zaeem

*Tse-Ming Yang is with graduate student of Aerospace Engineering, Tamkang University, Tamsui 251, Taiwan, ROC 492370365@s92.tku.edu.tw

†Fu-Yuen Hsiao is with faculty of Aerospace Engineering,Tamkang University, Tamsui 251, Taiwan, ROC fyhsiao@mail.tku.edu.tw

built a longitudinal flight dynamics with time-average theory [3], but only in 2-dimension space. In this paper, we intend to develop the three-dimensional model which will then be compared with the real trajectory.

In this research, we investigate the dynamics model of flapping MAV. Starting from Newton's second law we develop the equations of motion of our flapping-wing robot. Due to the fast flapping frequency compared with the translational and rotational rates, the average lift and thrust forces over each flapping period are applied to this model. Numerical simulations are also provided to examine the validity of our model and selected parameters.

2 Flapping MAV in TKU

The TKU MEMS Laboratory has been developing bird-like flapping MAVs for several years. Figure 1 demonstrates the most recent prototype, "*Golden Snitch*", which is a 7-gram-weight and 20-cm-wingspan aircraft including the fuselage, flapping wings, tail wing, battery, motor and a set of gear system. The flapping wing is driven by a motor with a four-bar linkage system, and its fabrication can be found in [2]. In *Golden Snitch* the stroke angle is designed around 53°.

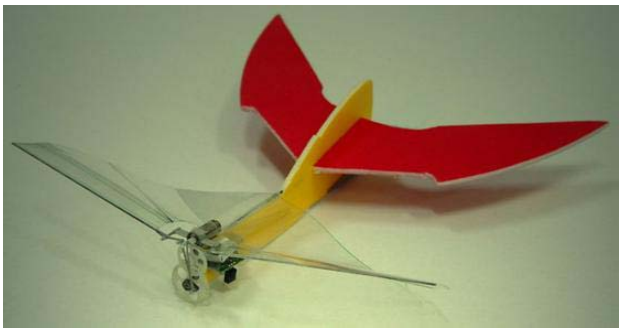

Figure 1: The flapping MAV developed by the TKU MEMS Lab

Currently *Golden Snitch* is remotely controlled by an Infrared Remote Controller. Constrained by the limitation of campus space and unskilled pilot, the flight duration is approximately 100 seconds. As a result, in order to extend the duration a large horizontal tail wing is designed to compensate the short of lift force from the main wing, and to stabilize the vehicle. Although the analysis in this paper is based on the current model of *Golden Snitch*, it can be extended to any other flapping wing robots in the future.

3 Dynamics Model

3.1 Definition of Frames

Before the discussion of the dynamics model, a suitable coordinate system should be defined first. A body-fixed frame is defined in Fig. 2. The x_b-axis points forward along the

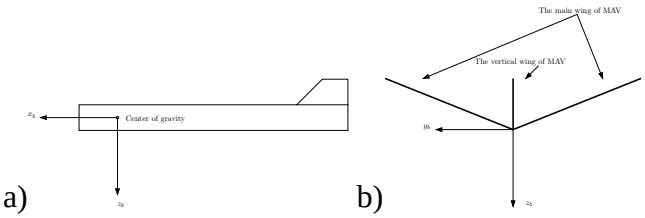

Figure 2: A cartoon showing the definition of the body-fixed frame.

axis of the fuselage in the MAV's plane of symmetry. The y_b-axis is normal to the plane of symmetry pointing in the direction of the right wing. The z_b-axis then points downward in the MAV plane of symmetry, completing the right-handed Cartesian system. In addition, the coordinates in the inertial frame are denoted as (x_f, y_f, z_f) in this paper. The transformation between these two frames can be accomplished by a rotational matrix $\mathbf{R}$, satisfying

$$\mathbf{V}_f = \mathbf{R}\mathbf{V}_b \quad (1)$$

$$\dot{\mathbf{R}} = \mathbf{R}\tilde{\omega} \quad (2)$$

where $\mathbf{V}_f$ and $\mathbf{V}_b$ denote any vectors in the inertial and body-fixed frames, respectively. $\tilde{\omega}$ is the cross product operator of the angular velocity $\vec{\omega} = (\omega_x, \omega_y, \omega_z)$ [8].

3.2 Equations of Motion

The equations of motion of the flapping wing MAV can be obtained by applying Newton's second laws, given by

$$\sum \mathbf{F} = m\frac{d}{dt}\mathbf{V} + \omega \times (m\mathbf{V}) \quad (3)$$

$$\sum \mathbf{M} = \mathbf{I}\frac{d}{dt}\vec{\omega} + \vec{\omega} \times (\mathbf{I}\vec{\omega}) \quad (4)$$

where $\mathbf{I}$ denotes the inertia tensor. The external forces includes the weight of the vehicle, aerodynamical forces by flapping wing, horizontal tail wing, and vertical tail. Those forces also generates moments about the center of gravity (CG). As a result, the expansion of Eqs. (3) and (4) can be found in [6] The components of forces and moments, F_{x_b}, F_{y_b}, F_{z_b} and M_{x_b}, M_{y_b}, M_{z_b}, are the force and moment along the x_b, y_b and z_b axis in the body-fixed coordinate system, respectively. The Euler angles can be computed from the rotation rates, given by:

$$\dot{\psi} = p + q\sin\psi\tan\theta + r\cos\phi\tan\theta \quad (5)$$

$$\dot{\theta} = q\cos\phi - r\sin\phi \quad (6)$$

$$\dot{\psi} = q\sin\psi\sec\theta + r\cos\phi\sec\theta \quad (7)$$

By solving Eqs. (3) and (4), the location, velocity and attitude of the MAV can be described as a function of time.

3.3 Averaging Theory and Formulation of Forces

3.3.1 Applicability of Averaging Theory

Due to the periodic motion of the flapping wings, the averaging theory is usually applied to analyze the dynamics of a flapping wing robot, such as in Refs. [3] and [8]. The averaging theory is applicable based on the assumption that the wing is much lighter than the the body. As a result, the flapping of the wing should not affect the vertical motion of the fuselage too much.

Even though the assumption sounds reasonable, it seems that no flight test data has been shown in the literatures. In [3] a control law is designed based on this assumption while in [8] a *ground-based* experiment has been designed to investigate the controllability of a biomimic MAV.

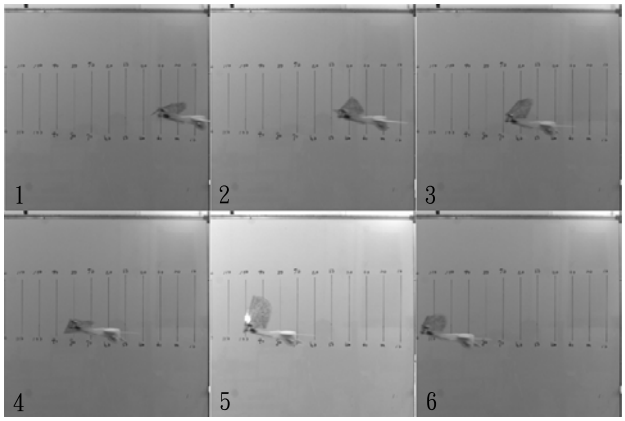

Figure 3: The cruise flight of *Golden Snitch* catched by high speed CCD camera.

Our *Golden Snitch*, however, verifies the validity of this assumption. As we can see in Fig. 3, *Golden Snitch* flies forward in a velocity of $\sim$3 m/s, but the fuselage still remains at an *almost* fixed height when the wings are flapping.

3.3.2 Averaged Force and Advance Ratio

In addition to the applicability of averaging theory, there was still one thing unclear before. Although the averaging theory was assumed to be applicable to the dynamical analysis of a flapping wing robot, the researchers in control field were still not clear about the formulation of the *averaged* lift and thrust forces. Accordingly, dynamics and control scientists usually simulated the lift and thrust force with a simple function, such as a periodic triangular wave.

On the other hand, the researchers in aerodynamics field always formulate the lift and thrust forces generated by a flapping wing as a function of the advance ratio, J, defined as

$$J = \frac{U}{2bf\Phi} \tag{8}$$

where Φ, f, and b are stroke angle, flapping frequency, and wing semi-span, respectively. Typically, unsteady-state flight has advance ratio J less than 1. Low advance ratio J is an indication that these flyers must flap their wings at high speed compared to the speed of their flights in order to stay aloft. Therefore, the regime of $J < 1$ is dominated by unsteady-state flight. On the other hand, for $J \gg 1$, the flight regime becomes quasi-steady and approaches steady-state. For example, a fixed-wing airplane operates in the regime of J near infinite because the wings' flapping frequency is zero. The lift and thrust forces can be expressed as functions of J [2]

$$F_{\text{lift}} = \frac{1}{2}\rho U^2 S C_L(J) \tag{9}$$

$$F_{\text{thrust}} = \frac{1}{2}\rho U^2 S C_T(J) \tag{10}$$

where $C_L(J)$ and $C_T(J)$, as functions of J, denote the lift coefficient and thrust coefficient, respectively.

Here we claim that *the forces calculated from the lift or thrust coefficient as a function of J can be treated as the averaged force*. A simple proof goes below. Consider a very

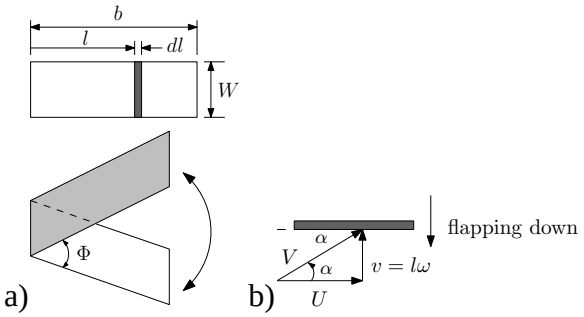

Figure 4: A cartoon showing the definition of wing parameters.

thing rectangular wing, as shown in Fig. 4(a), with length b, width W, stroke angle Φ, and flapping frequency $\omega = 2\pi f$. Assume the setting angle is zero so that the angle of attack (AOA) is determined by the attacking angle of the incoming air stream completely. Consider a small area element on the wing, whose flapping motion is shown in Fig. 4(b). According to aerodynamics theory, the lift force generated by this element is formulated as

$$dF = \frac{1}{2}\rho V^2 C_L(\alpha) dA \tag{11}$$

where $V^2 = U^2 + (l\omega)^2$, $dA = W dl$, and

$$\alpha = \arctan\left(\frac{l\omega}{U}\right)$$

To simply the notation we define $l/b = \gamma$. Introducing the advance ratio we obtain

$$l\omega = \frac{\gamma\pi}{J\Phi} U$$

As a result, Eq. (11) can be reformulated as

$$\begin{aligned} dF &= \frac{1}{2}\rho V^2 C_L(\alpha) dS \\ &= \frac{1}{2}\rho U^2 Wb \left[1 + \left(\frac{\pi}{J\Phi}\right)^2 \gamma^2\right] C_L(\alpha) d\gamma \\ &= \frac{1}{2}\rho U^2 S \left[1 + \left(\frac{\pi}{J\Phi}\right)^2 \gamma^2\right] C_L(\alpha) d\gamma \end{aligned} \tag{12}$$

where $S = Wb$ is the total area of the wing, and $\alpha = \alpha(J, \gamma)$. Consider the average force during the downstroke during time interval T_d, given by

$$\begin{aligned} \bar{F} &= \frac{1}{T_d}\int_0^{T_d} F(t) dt \\ &= \frac{1}{T_d}\int_0^{T_d}\int_0^{F} dF\, dt \\ &= \frac{\rho U^2 S}{2T_d}\int_0^{T_d}\int_0^{1} \left[1 + \left(\frac{\pi}{J\Phi}\right)^2 \gamma^2\right] C_L(\alpha) d\gamma\, dt \end{aligned}$$

Since the integrant is not an explicit function of time, we can integrate with respect of time first and null out T_d. Therefore,

$$\bar{F} = \frac{\rho U^2 S}{2}\int_0^{1} \left[1 + \left(\frac{\pi}{J\Phi}\right)^2 \gamma^2\right] C_L(\alpha(J, \gamma)) d\gamma$$

Define

$$C'_L(J) = \int_0^{1} \left[1 + \left(\frac{\pi}{J\Phi}\right)^2 \gamma^2\right] C_L(\alpha(J, \gamma)) d\gamma$$

We obtain that

$$\bar{F}_d = \frac{1}{2}\rho U^2 S C'_{L_d}(J) \tag{13}$$

where the subscript d denotes *downstroke*. Similarly, the average force during the upstroke is given by

$$\bar{F}_u = \frac{1}{2}\rho U^2 S C'_{L_u}(J) \tag{14}$$

As a result, the average force generated during a complete flapping is given by

$$\begin{aligned} \bar{F} &= \bar{F}_d + \bar{F}_u \\ &= \frac{1}{2}\rho U^2 S C'_{L_d}(J) + \frac{1}{2}\rho U^2 S C'_{L_u}(J) \\ &= \frac{1}{2}\rho U^2 S C'_L(J) \end{aligned} \tag{15}$$

where $C'_L(J) = C'_{L_d}(J) + C'_{L_u}(J)$. We can see that the average force has the same formulation as Eqs. (9) and (10).

We would admit that this is not a rigorous proof because many aerodynamics factors are not considered, such as the stability of the air flow, the flexibility of the wing and so on. However, at least this proof gives a qualitative link between the average force used in the dynamics field and the most common way to formulate flapping lift and trust forces in the aerodynamics field. In other words, if we have the lift and thrust coefficient curves at hand, which are usually easy to obtain in aerodynamics journals, we can simply apply the same methodology of analyzing a fixed-wing vehicle to the analysis of a flapping-wing robot.

3.4 Formulation of Forces and Moments

Having shown that the average forces over one flapping period can be calculated by using Eqs. (9) and (10), which is independent of time, we conclude that the methodology to analyze a fixed wing vehicle can be applied to the flapping wing vehicle. There are only two differences. First of all, the force coefficients C_L and C_T are no longer functions of angle of attack only, but also functions of advance ration. Second, when applied to analyze the dynamics of the whole vehicle, we don't use angle of attack since it is not rigorously defined in flapping motion. Instead, the set angle and stroke angle are introduced.

Figure 5 provides the distribution of aerodynamics forces on the wing. As a result, provided Eqs. (9) and (10) F_{x_b} and F_{z_b} can be obtained by considering the vector addition of the lift and thrust forces.

$$F_{z_{b_{wing}}} = F_{thrust}\sin(\alpha) - F_{lift}\cos(\alpha) \quad (16)$$

$$F_{x_{b_{wing}}} = F_{thrust}\cos(\alpha) + F_{lift}\sin(\alpha) \quad (17)$$

where α is set angle of MAV.

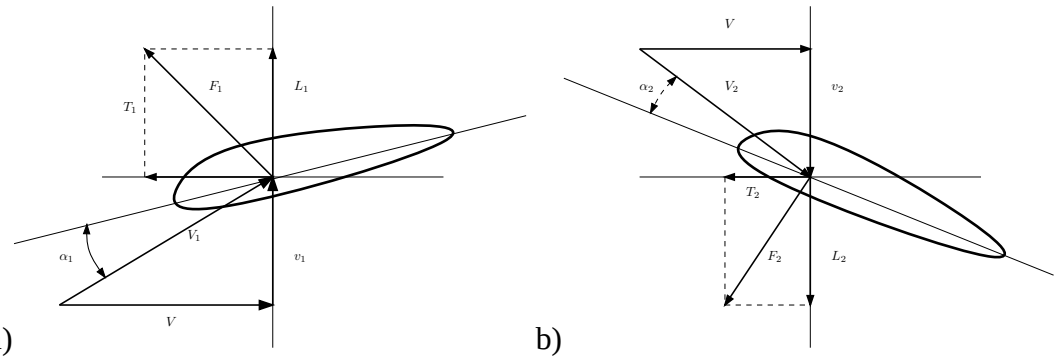

Figure 5: The aerodynamic force distribution during downstroke and upstroke.

On the other hand, the moments exerted on the MAV can be obtained through summing up all individual moment and torque. All the necessary geometric parameters to calculate moments are shown in Fig. 6. In addition to the regular formulation of moments, one thing to remind again is that we have to consider the torque applied by the motor,

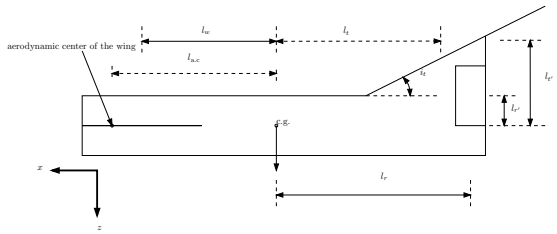

Figure 6: A cartoon showing the geometric parameters of the fuselage.

Set angle	10°	20°	30°	40°	50°
a	19.07	20.22	35.35	42.09	58.25
b	5.471	4.174	4.851	4.823	6.107
c	0.6914	1.181	1.404	2.051	2.346
a'	109.8	103.9	153.2	156.2	92.43
b'	7.878	8.168	11.05	10.58	9.154
c'	0.3139	0.1475	0.01054	-0.5002	-0.8389

Table 1: The parameters in force coefficients for a flapping wing.

$\tau = \tau_{\text{motor}}$ pointing along $+x_b$-axis because our motor spins clockwise. Applying the formulated forces and moments to Eqs. (3) and (4) we can solve for the position, velocity and attitude of the MAV.

4 Flight Test and Numerical Simulation

Having shown that the averaging theory is applicable to the flapping wing MAV, and the way to obtain the average forces from experiment data, we apply this result to the analysis of our *Golden Snitch*.

4.1 Coefficients of the Main Wing

According to Ref. [1], the coefficient of lift and coefficient of thrust can be modeled as:

$$C_{L_{wing}} = ae^{-bJ} + c \tag{18}$$

$$C_{T_{wing}} = a'e^{-b'J} + c' \tag{19}$$

For the TKU flapping MAV, those parameters are obtained through wind tunnel test, and list as a function of set angle in Tab. (1). With the lift and thrust coefficients, the forces can be obtained using Eqs. (9) and (10). According to the result from the proceeding section, the obtained forces will be the average ones over one flapping period. An example showing the variation of forces as a function of time is shown in Figs. 7 and 8.

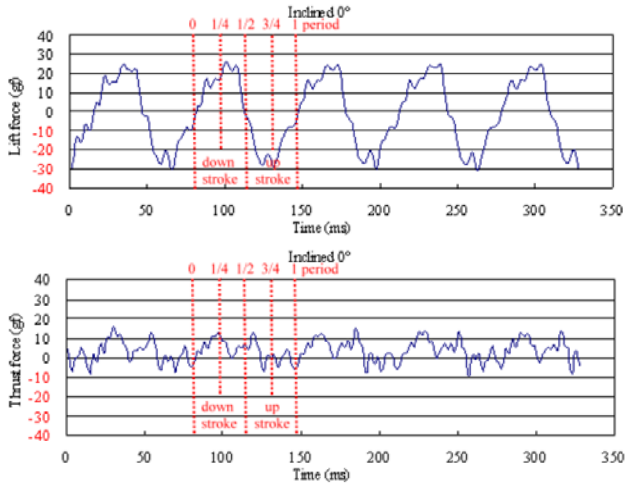

Figure 7: The variation of lift and thrust forces during a flapping period.

4.2 Coefficients of the Horizontal Wing

In addition to the main wing, there are still two other wings, the vertical and the horizontal wing, should be considered. Since these two wings are fixed, the conventional aerodynamics theory can be applied.

Although the most confidential way to obtain the force coefficients of the vertical and tail wings is to do the wind tunnel test, in the preliminary analysis we introduce the so called "Prandtl's Theory" This practical theory to predict the aerodynamic properties of a finite wing was developed by Ludwig Prandtl and his colleagues. Different from airfoil theory, dealing with an infinite wing, a finite wing is considered so that the induced drag is revealed in this theory too,

$$C_{D,i} = \frac{C_L^2}{\pi \mathrm{AR}} \tag{20}$$

Eq. (20) is an important result. It states that the induced drag coefficient is directly proportional to the square of the lift coefficient. Hence, induced drag is intimately related to the production of lift on a finite wing; indeed, induced drag is frequently called the drag due to lift. Another important aspect of induced drag is evident in Eq. (20); that is, $C_{D,i}$ is inversely proportional to aspect ratio. Hence, to reduce the induced drag, we want a finite wing with the highest possible aspect ratio.

In our tail wing, we select a wing whose shape is showed in Fig. 9. It is a back swept wing, and the coefficient of lift can be derived as

$$C_{L_{tail}} = \frac{2\pi \cos \Lambda}{\sqrt{1+P^2}+P} \alpha_{tail} \tag{21}$$

where

$$P = \frac{2\pi \cos \Lambda}{\pi \mathrm{AR}},$$

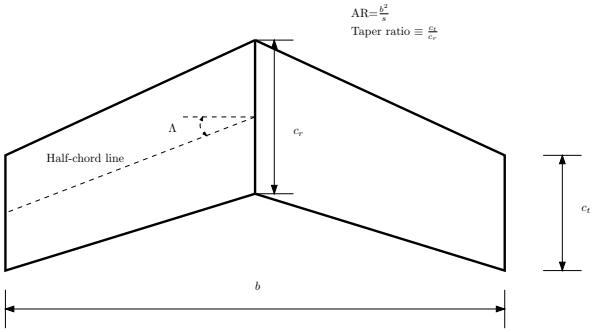

Figure 8: The shape of tail wing

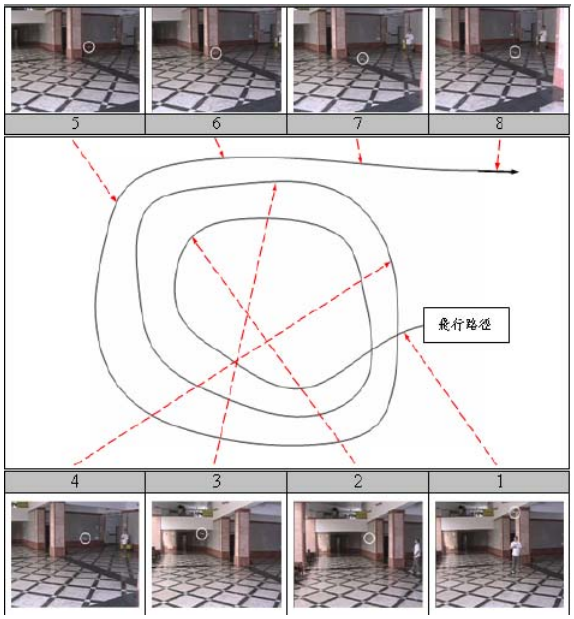

Figure 9: An example of the flight test trajectory

Λ is the sweep angle of the half-chord line of the wing, α_{tail} is the angle of attack of tail wing, and AR defined as

$$\mathrm{AR} = \frac{b^2}{S} \tag{22}$$

Those parameters of the *Golden Snitch* are given as follows: $b = 0.15$ m, $c_r = 0.035$ m, $c_t = 0.02$ m, $\Lambda = 28°$. Similarly, the same method also applies to simulate the property of the vertical wing. In order to simplify this problem, the force is assumed to exert on the aerodynamic center of the vertical wing as usually done in conventional analysis.

4.3 Flight Test

As mentioned earlier, the *Golden Snitch* has been put into flight test and its flight duration is about 100 seconds. An example of the flight trajectory is shown in Fig. 10. The only control

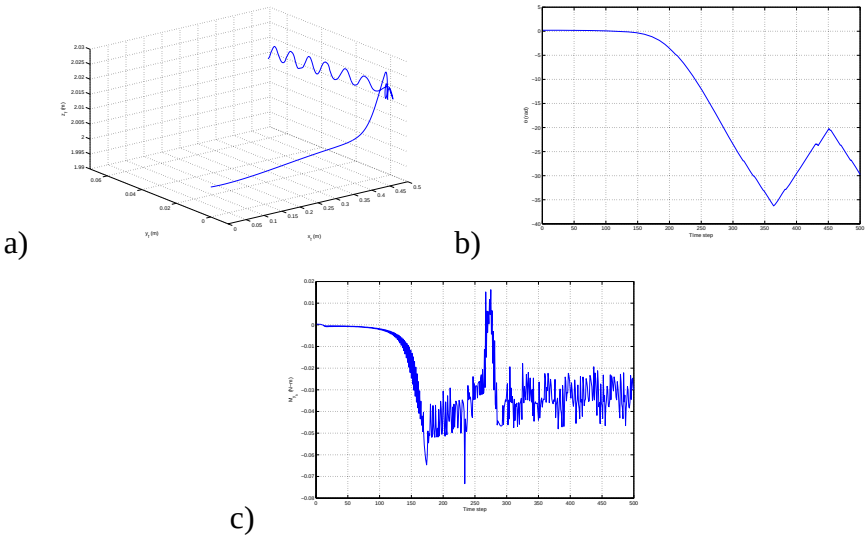

Figure 10: The flight trajectory in case 1.The time history of pitch angle $(\theta)M_{y_b}$ in case 1.

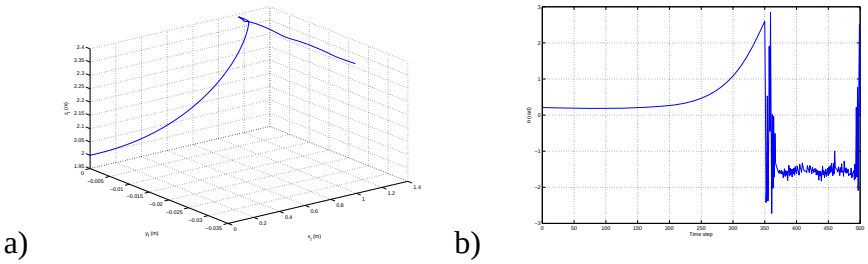

Figure 11: The flight trajectory in case 2.

applied to this vehicle is the torque of the motor, which controls the flapping frequency. In other words, there is no control of direction. The flight trajectory, however, is spiral. This is resulted from the torque generated by the motor due to the conservation of angular momentum.

4.4 Numerical Simulation

4.4.1 Attitude Equilibria at Cruise Flight

At cruise flight the MAV must be in the equilibria of its attitude. According to our model, we obtain that the pitch angle at cruise flight must be $12°$. Examining Fig. 3 we realize that the *Golden Snitch* flies at the angle of $15°$. This is encouraging since our prediction is quite close to the reality. However, this fact also implies that the predicted lift force at wing tail may be too large so that the pitch angle is smaller than the real one. This fact will later on affect the simulation of flight trajectory.

4.4.2 Simulated Flight Trajectories

Two cases are simulated so far, shown in Figs. 11-**??** and a time step is 0.001 seconds. In the first case we use the derived parameters from the previous chapter. However, the trajectory diverges in about 0.15 seconds. The simulation results are provided in Figs. 11-**??**. The results in Figs. **??** and **??** seem to imply that tail force is too large so that the vehicle is subject to a continuous negative pitch torque. To correct the result, we reduce the lift coefficient of the tail wing in the second case.

4.4.3 Discussion

In the simulation of case 1, the moment in y_b direction is nearly negative. It cause the MAV nose-down and it is obvious against to the real flight. The possible reasons are still under in investigation. For example the aerodynamic center of flapping and tail wing is unknown, therefore a guessed value is used in the simulation. The lift and drag coefficients of tail wing are also an important factor to make the result unreasonable. In the previous section, we apply the Prandtl's classical lifting-line theory to study the tail wing. However, the tail wing located after the flapping wing is in an unsteady flow, so there might be errors in our prediction.

In case 2, the attitude stays reasonable for a longer time. Moreover, the MAV has the trend to fly a clockwise spiral trajectory. However, due to the lack of experimental data, we are not aware of the stall condition of a flapping wing. This causes the lift force grows sharply and eventually diverge the trajectory. As a result, abundant the experiment database and more knowledge of flapping aerodynamics would be two important future work in this project.

5 Conclusions

In this paper we study the dynamics of a flapping wing MAV. Our results are also compared with the flight test data, using the flapping wing MAV developed by TKU MEMS Lab. Starting from Newton's second law, we derive the equations of motion for the MAV. By observing the cruise flight of our MAV in the high speed CCD Camera, we show that flapping doesn't affect the vertical motion of the whole vehicle, implying that the averaging theory is applicable. We also analytically prove that the time-average forces (lift and thrust) have the same formulation as those in the conventional fixed wing, while the only difference is the coefficient of lift, which is a function of advance ratio and set angle instead of angle of attack. As a result, having the force coefficient curves from wind tunnel test data, we can simulate the dynamics immediately without assuming the time history of those aerodynamics forces. Numerical simulations are also provided in this paper. Our numerical simulations not only catch the trend of the flight test trajectory, but also match the cruise flight condition. Due to the lack of experimental data, the simulations don't exactly match the flight test data yet. As a result, abound with experimental database and knowledge of flapping aerodynamics would be two important future work for the built of

complete dynamical model.

6 Acknowledgement

The work described here is funded by the National Science Council through project NSC 96-2221-E-032-015. The authors wish to thank Dr. Lung-Jieh Yang and his research group for providing flight test and wind tunnel test data.

References

[1] M.H. Dickinson, F.O. Lehmann, and S.P. Sane, "Wing rotation and the aerodynamic basis of insect flight," *Science*, Vol. 284, pp. 1954-1960, 1999

[2] C. K. Hsu, *The Preliminary Design, Fabrication, and Testing of Flapping Micro Aerial Vehicles*, Ph.D. Dissertation, Tamkang University, 2008

[3] Z.A. Khan, and S.K. Agrawal, "Control of Longitudinal Flight Dynamics of a Flapping-Wing Micro Air Vehicle Using Time-Averaged Model and Differential Flatness Based Controller," *Proceedings of the 2007 American Control Conference*, pp. 5284-5289, 2007

[4] Dae-Kwan Kim, and Jae-Hung Han, "Smart flapping wing using Macro-Fiber Composite actuators," Proceeding of Smart Structures and Materials, 2006

[5] U.M. Norberg, *Vertebrate Flight: Mechanics, Physiology, Morphology, Ecology and Evolution*, Springer-Verlag, 1990

[6] W.F. Phillips, *Mechanics of Flight*, John Wiley & Sons, 2004

[7] T. Rakotomamonjy, M. Ouladsine, and T. Le Moing, "Modelization and Kinematics Optimization for a Flapping-Wing Microair Vehicle," *Journal of Aircraft*, Vol. 44, 2007

[8] L. Schenato, D. Campolo, and S. Sastry, "Controllability issuse in flapping flight for biomimic MAVs," *Proceedings of the 42nd IEEE Conference on Decision and Control*, pp. 6441-6447, 2003

[9] M. Sun, J. Wang and Y. Xiong, "Dynamic flight stability of hovering insects," *Acta Mechanica Sinica*, 2007

[10] J. Yan, R.J. Wood, S.S. Avadhanula, , R.S.M. Fearing, "Towards flapping wing control for a micromechanical flying insect," *IEEE International Conference on Robotics and Automation*, 2001